Proceedings of the 6th International Conference on Nanostructures (ICNS6)
7-10 March 2016, Kish Island, Iran

Morphology, structure and optical properties of low bandgap organic-inorganic halide perovskite based on $CH_3NH_3Sn_xPb_{1-x}I_3$

Mojtaba Abdi-Jalebi[a]*, Aditya Sadhanala[a], Richard H. Friend [a]*

[a] Cavendish Laboratory, University of Cambridge, JJ Thomson Avenue, Cambridge CB3 0HE, United Kingdom.
*ma571@cam.ac.uk, rhf10@cam.ac.uk

Abstract: Herein, we investigate morphology, structure and optical properties of low band gap organic-inorganic halide perovskite based on a mixture of lead and tin as the divalent cation in ABX_3 structure. A significant change in morphology of $CH_3NH_3Sn_xPb_{1-x}I_3$ perovskite with x as well as an alteration in crystal structure from I4cm (β-phase) to pseudocubic P4mm (α-phase) space groups is observed when Sn is the dominant divalent cation ($x \geq 0.5$). Photo thermal defection optical absorption spectroscopy (PDS) and photoluminescence (PL) of $CH_3NH_3Sn_xPb_{1-x}I_3$ show the non-linear change in the band edge of perovskite. The bandgap as low as 1.17 eV and the most red-shifted PL at 1035nm is achieved for perovskite with x=0.8. In addition, higher electronic disorder is measured for $CH_3NH_3Sn_xPb_{1-x}I_3$ compounds with higher x.

Keywords: Low bandgap perovskite; $CH_3NH_3Sn_xPb_{1-x}I_3$; Photothermal deflection spectroscopy

Introduction

One of the main concerns with organo-metal lead halide perovskite is the toxicity of lead, and therefore, a key scientific challenge is to replace or diminish the lead in the perovskite crystal with a less toxic metal. According to the recent studies, tin (Sn) become the most viable replacement for Pb in perovskite materials. However, Sn based perovskite materials still has relatively low PCE (6.4%) and V_{oc} (0.88 V) [1]. Recently, several groups have reported different solution processing methods to prepare mixed Sn and Pb perovskites $CH_3NH_3Sn_xPb_{1-x}I_3$ in order to achieve tunable band gap and high carrier mobilities [2-4]. Particularly, Ogomi et al. [3] reported a linear reduction of band gap with increasing the Sn content, while Hao et al. observed a nonlinear relationship between the band gap and the content of Sn [4]. Stoumpos et al. show that samples prepared from different solution-processing methods can give rise to very different optical performance, resulting in different relationships between the Pb/Sn ratio and band gap [2].

In this study, we propose to synthesize low band-gap organo-metal halide perovskites based on a mixture of Sn and Pb and investigate morphology, structure and optical properties of them. Therefore, a series of lead and tin mixture perovskite were synthesized and their morphology and crystal structure were explore using field emission scanning electron microscope (FE-SEM) and X-ray diffraction (XRD), respectively. In addition, optical properties of them were studied by PL and PDS.

Materials and method

Unless stated otherwise, all materials were purchased from Sigma- Aldrich or Acros Organics and used as received. CH_3NH_3I was synthesized according to a reported procedure [5]. A bright yellow solution of pure lead ($CH_3NH_3PbI_3$) and tin ($CH_3NH_3SnI_3$) perovskite were prepared by dissolving stoichiometric amounts of CH_3NH_3I and MX_2, (M = Sn, Pb) in DMF at one $mol.L^{-1}$ concentration. In order to make mixture of lead and tin based perovskite compounds ($CH_3NH_3Sn_{1-x}PbxI_3$), the pure solution of them were mixed in different ratio. These solution were then spin coated on either a spin coated TiO_2 on a FTO-coated glass or spectrosil at 4000 rpm for 60 s and dried at 100 ^{0}C for 15 min to remove the solvent.

Results and Discussion

As it is mentioned in the experimental part, a series of Pb and Sn mixture perovskite ($CH_3NH_3Sn_xPb_{1-x}I_3$) including $CH_3NH_3Sn_{0.2}Pb_{0.8}I_3$ (20Sn), $CH_3NH_3Sn_{0.4}Pb_{0.6}I_3$ (40Sn), $CH_3NH_3Sn_{0.6}Pb_{0.4}I_3$ (60Sn), $CH_3NH_3Sn_{0.8}Pb_{0.2}I_3$ (80Sn) were synthesize by mixing different ratio of $MAPbI_3$ and $MASnI_3$. It is notable that the $CH_3NH_3SnI_3$ and $CH_3NH_3PbI_3$ are phrased as 100Sn and 100Pb, respectively.

Morphological Characterization

To compare the surface morphology of different mixtures of $CH_3NH_3Sn_xPb_{1-x}I_3$ deposited on mesoporous TiO_2 photoanode, field emission scanning electron microscopy (FESEM) is employed (Fig. 1). The $CH_3NH_3PbI_3$ film is composed of interconnected nanoscale domains with sizes ranging from 200 to 500 nm with decent film coverage and needle like structures, which are the same as those reported previous work [3]. However, the 20Sn film displays better film quality and coverage in which wider needles form. This markedly increased film coverage ensures connectivity between grains, which is

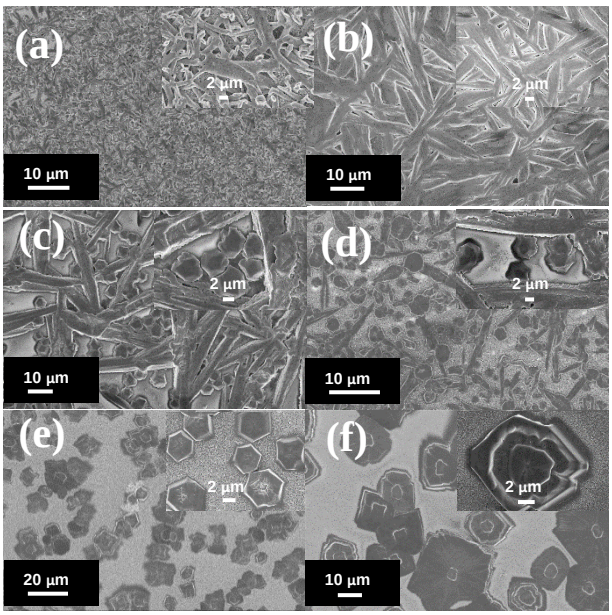

Fig. 1. Top-view SEM images of (a) 100Pb, (b) 20Sn, (c) 40Sn, (d) 60Sn, (e) 80Sn and (f) 100Sn perovskite films deposited on a mesoporous TiO_2-coated FTO.

crucial to mitigate short-circuiting, charge leaking, and charge trapping at the crystalline boundaries. Further increase in Sn content lead to appearance of hexagonal shape crystals in between the needles as can be seen in the SEM image of 40Sn and 60Sn (Fig. 1 c, d). Surprisingly, in the 80Sn and 100Sn films, the needle like crystals completely disappear and large, 3-5 µm, randomly oriented flowerlike crystals appear. It is notable that the surface coverage in these films decrease significantly.

Structural Characterization

To investigate the crystal structure of $CH_3NH_3Sn_xPb_{1-x}I_3$ perovskite, X-ray diffraction spectroscopy was carried out. The $CH_3NH_3Sn_xPb_{1-x}I_3$ adopts the perovskite structure type (ABX_3) consisting of corner-sharing $[Sn_{1-x}Pb_xI_6]^{-4}$ octahedra in which the metal site is randomly occupied by either Sn or Pb atoms and the A cation is selected to balance the total charge. It is notable that $CH_3NH_3SnI_3$ and $CH_3NH_3PbI_3$ crystallize in the pseudocubic P4mm (α-phase) and tetragonal I4cm (β-phase) space groups, respectively, at ambient conditions. It is reported that $CH_3NH_3PbI_3$ undergoes a reversible structural phase transition to the P4mm space group becoming isostructural to its Sn analogue at higher temperatures (~330K) [2].

Identical structural transition can be also realized in the $CH_3NH_3Sn_xPb_{1-x}I_3$ for an $x \geq 0.5$ value at room temperature. It is obvious from the X-ray diffraction patterns in Fig. 2 that the two peaks within the range between 22°−25° 2θ ($x < 0.5$), which could be indexed to

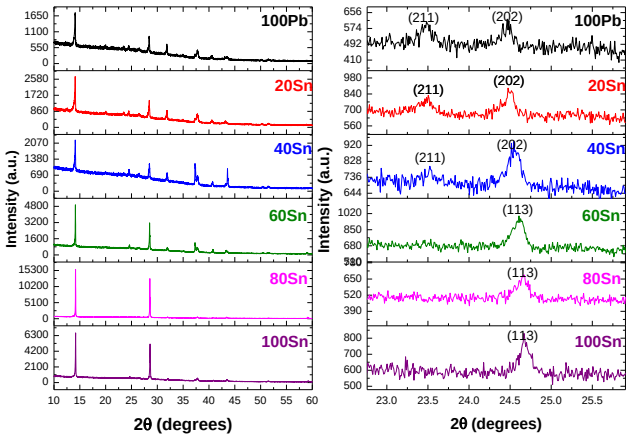

Fig. 2. X-ray diffraction spectra of $CH_3NH_3Sn_xPb_{1-x}I_3$ where x=0, 0.2, 0.4, 0.6, 0.8 or 1. The right side XRD shows the structural transition from tetragonal I4cm (β-phase) to pseudocubic P4mm (α-phase) space groups happening for x>0.5.

(211) and (202) planes in the tetragonal I4cm space group, can gradually merge to a single peak corresponding to the (113) plane in the P4mm space group when x becomes >0.5 due to the higher symmetry of P4mm [2].

According to the Scherrer equation, the mean size of the crystallite is inversely proportional to the full width half the maximum (FWHM) of the XRD peak intensity of the material. Thus, the crystallite size for $CH_3NH_3Sn_xPb_{1-x}I_3$ is increased for the perovskite containing higher amount of Sn with the exception of 80Sn which has the lowest FWHM.

Photothermal deflection spectroscopy (PDS)

We used PDS to explore the optical absorption of the synthesized $CH_3NH_3Sn_xPb_{1-x}I_3$ perovskite near the band edge (Fig. 3). A clear red shift in the band edge of perovskite based on Pb and Sn mixture is observed for x>0. Notably, by stoichiometrically mixing the divalent metal iodides of Sn and Pb with methylammonium iodide, we can easily synthesize the $CH_3NH_3Sn_xPb_{1-x}I_3$ solid solutions with a bandgap tunable between 1.17 and 1.55 eV. The intermediate compounds with x = 0.8 and 0.6 show the smallest bandgaps of 1.17 eV. It is important to note that the optimal bandgap for a single-junction solar cell is between 1.1 and 1.4 eV, currently beyond the range of most investigated methylammonium lead trihalide systems. The $CH_3NH_3Sn_xPb_{1-x}I_3$ series is therefore promising for more efficient photovoltaic devices for both the single junction and also tandem architecture device where the optimum bandgap for a bottom cell lies in around 1 eV [6]. It is also apparent that the above bandgap absorption of 100Pb, 20Sn and 40Sn

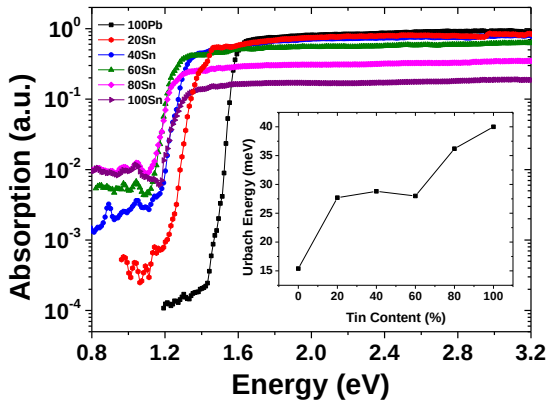

Fig. 3. The absorption spectra of the synthesized $CH_3NH_3Sn_xPb_{1-x}I_3$ serial compounds measured using the PDS technique. The inset shows the corresponding Urbach energies for all samples. The error bar is defined by the s.d.

are higher compare to the other compounds. This is mostly due to the better surface coverage of these film as we observed in SEM images (Fig. 1). In addition, the absorption tail shifts up by increasing the content of tin which can be attributed to the oxidation of $CH_3NH_3Sn_xPb_{1-x}I_3$ compounds. Oxidation of Sn based compounds happened during the PDS measurement since there is a certain amount of oxygen inside the FC72 liquid which is used as a heat transfer medium for the sample.
Urbach energy 'E_u' as the slope of the exponential part of the Urbach tail gives an estimation about the concentration of defects and level of electronic disorder [7]. The estimated Urbach energies for $CH_3NH_3Sn_xPb_{1-x}I_3$ serial compounds and their corresponding data fittings are shown in the inset of Fig. 3. These values suggest that the $CH_3NH_3Sn_xPb_{1-x}I_3$ compounds with higher amount of tin have a higher level of electronic disorder.

Photoluminescence study

Steady state PL spectra of $CH_3NH_3Sn_xPb_{1-x}I_3$ serial compounds are presented in Fig. 4. A clear red shift of PL

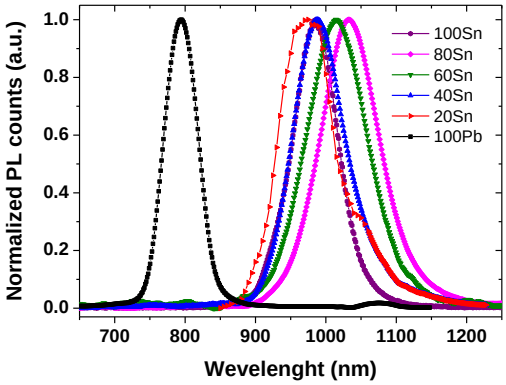

Fig. 4. Photoluminescence spectra of $CH_3NH_3Sn_xPb_{1-x}I_3$ serial compounds.

is observed for all Sn contained perovskite compound compared to the $CH_3NH_3PbI_3$ which shows a narrow peak at 795nm. The intermediate compounds with x = 0.8 and 0.6 show the highest red shift and PL peak at 1015nm and 1035nm, respectively. It is notable that the position of PL peak for 100Sn and 40Sn is identical while the 40Sn shows a broader peak to the red. In addition, the PL peak for 20Sn sample represent a slight blue shift in comparison with the 100Sn. The PL data are consistent with the PDS data in which the intermediate compounds with lower band-gap have the most red-shifted absorption edge.

Conclusions

We have synthesized low bandgap perovskite (e.g. 1.17eV) using the alloyed perovskite solid solutions of methylammonium lead iodide ($CH_3NH_3PbI_3$) and its tin analogue ($CH_3NH_3SnI_3$). The morphology of $CH_3NH_3Sn_xPb_{1-x}I_3$ alter significantly with x consisting needlelike or flowerlike crystals or a mixture of them. A structural transition from tetragonal I4cm (β-phase) to pseudocubic P4mm (α-phase) space groups is realized in the $CH_3NH_3Sn_xPb_{1-x}I_3$ for $x \geq 0.5$ using XRD. In addition, the crystallite size is increased significantly by raising the content of Sn in the perovskite structure. The significant red shift of bandgap is measured for the intermediate compounds with x = 0.8 and 0.6 which shows the smallest bandgap of about 1.17 eV using PDS. Moreover, the values for Urbach energy suggest that the $CH_3NH_3Sn_xPb_{1-x}I_3$ compounds with higher amount of tin have a higher level of electronic disorder. Photoluminescence spectroscopy further confirm the red-shift in the bandgap of intermediate compounds of $CH_3NH_3Sn_xPb_{1-x}I_3$ in which a PL peak at 1035 is observed for x=0.8.

Acknowledgment (Optional)

MAJ thanks Nyak technology Ltd for PhD funding.

References

[1] Hao, F.; Stoumpos, C. C.; Cao, D. H.; Chang, R. P. H.; Kanatzidis, M. G. *Nat. Photonics* 2014, 8, 489−494.

[2] Stoumpos, C. C.; Malliakas, C. D.; Kanatzidis, M. G. Inorg. Chem. 2013, 52, 9019−9038.

[3] Hao, F.; Stoumpos, C. C.; Chang, R. P. H.; Kanatzidis, M. G. J. Am. Chem. Soc. 2014, 136, 8094−8099.

[4] Ogomi, Y.; Morita, A.; Tsukamoto, S.; Saitho, T.; Fujikawa, N.; Shen, Q.; Toyoda, T.; Yoshino, K.; Pandey, S. S.; Ma, T.; Hayase, S. J. Phys. Chem. Lett. 2014, 5, 1004−1011.

[5] Kim, H.-S. *et al*. *Sci Rep* 2, 591 (2012).

[6] Meillaud, F.; et. al ; Miazza, C. Sol. *Energy Mater. Sol. C* 2006, 90, 2952.

[7] Sadhanala, A.; et. al; Friend, R. H. *J. Phys. Chem. Lett*. 2014, 1–5.